Astrophys Space Sci (2007) 307:115–119
DOI 10.1007/s10509-006-9255-0

ORIGINAL ARTICLE

Assessing Mix Layer Amplitude in 3D Decelerating Interface Experiments

C. C. Kuranz · R. P. Drake · T. L. Donajkowski · K. K. Dannenberg · M. Grosskopf · D. J. Kremer · C. Krauland · D. C. Marion · H. F. Robey · B. A. Remington · J. F. Hansen · B. E. Blue · J. Knauer · T. Plewa · N. Hearn

Received: 21 April 2006 / Accepted: 20 September 2006

Abstract We present data from recent high-energy-density laboratory experiments designed to explore the Rayleigh–Taylor instability under conditions relevant to supernovae. The Omega laser is used to create a blast wave structure that is similar to that of the explosion phase of a core-collapse supernova. An unstable interface is shocked and then decelerated by the planar blast wave, producing Rayleigh–Taylor growth. Recent experiments were performed using dual, side-on, x-ray radiography to observe a 3D "egg crate" mode and an imposed, longer-wavelength, sinusoidal mode as a seed perturbation. This paper explores the method of data analysis and accurately estimating the position of important features in the data.

Keywords Rayleigh-Taylor instability · Supernova · Laboratory astrophysics

Introduction

In 1987, a core-collapse supernova (SN) occurred ∼160000 light years away, making it the closest SN in modern times. The proximity of SN1987A made it possible to use contemporary astronomical instruments to collect data from the SN. At the time, existing models did not agree with the data collected, specifically, the high velocities and early x-ray emission of dense core elements. These discrepancies motivated improvement of the understanding of core-collapse SNe. Current models have started to explain the mysteries of SN1987A, but many questions remain unanswered. Of particular interest is the effect of hydrodynamic instabilities on the transport of the heavy core elements.

High Energy Density (HED) facilities make it possible to study specific, well-scaled areas of astrophysical phenomena, in our case, the blast-wave-driven interface of a core-collapse supernova. Intense lasers can create the extremely large energies in mm-scale targets previously seen only in astrophysical systems. Experiments of this type have been done or are planned at numerous laser facilities (Drake et al., 2004; Kane et al., 2000; Robey et al., 2001; Remington et al., 2000). It is possible to compare the SN and the experiment because the targets can be well-scaled to the SN explosion phase so that the two will have similar hydrodynamic evolution (Ryutov et al.,1999).

The Rayleigh–Taylor (Rayleigh, 1900; Taylor, 1950) instability occurs when a system has a density gradient and effective pressure gradient in opposing directions. This is the case both the SN, where a blast wave propagates from the dense core through less dense, outer layers of the star, and in the laboratory experiment, where a planar blast wave moves through a dense plastic layer into a less dense foam layer. The resulting evolution is the flow of dense elements "sinking" outward in the form of fingers or spikes. Also, the less dense material "floats" inward and is referred to as bubbles.

Experiments

During the experiment ten Omega (Boehly et al., 1995) laser beams irradiate a 150 μm layer of polyimide of a density

C. C. Kuranz (✉) · R. P. Drake · T. L. Donajkowski · K. K. Dannenberg · M. Grosskopf · D. J. Kremer · C. Krauland · D. C. Marion
University of Michigan, Ann Arbor, MI, USA

H. F. Robey · B. A. Remington · J. F. Hansen · B. E. Blue
Lawrence Livermore National Laboratory, Livermore, CA, USA

J. Knauer
University of Rochester, Rochester, NY, USA

T. Plewa · N. Hearn
University of Chicago, Chicago, IL, USA

1.41 g/cc. The total energy of the beams is ∼5 kJ and the irradiance is $\sim 10^{15}$ W/cm^2, producing an ablation pressure of ∼50 Mbars, which creates a strong shock in the plastic layer of the target. After 1 ns, the laser pulse ends, causing the material to rarify. When the rarefaction wave overtakes the shock wave, a planar blast wave is formed. After about 2 ns, the blast wave crosses an interface between the plastic and carbonized resorcinol formaldehyde (CRF) foam. The foam has a density of 50 mg/cc, making the density drop between the plastic and foam similar to that expected in the case of the H/He interface in SN1987A. The interface is initially accelerated by the blast wave and then decelerated over a long period of time by the foam layer. The interface is unstable to both Richtmeyer-Meshkov (Richtmyer, 1960; Meshkov, 1969) and Rayleigh–Taylor instabilities. However, interface growth due to Rayleigh–Taylor dominates after the first few nanoseconds.

Diagnostics

This experiment uses an ungated Static Pinhole Camera Array (SPCA) loaded with Direct Exposure Film (DEF) behind Be, plastic and Ti or Sc light shields. To protect the ungated diagnostic from laser beams and hot plasma created during the experiment, a large gold shield is part of the target structure. The polyimide and foam components are placed inside a polyimide tube and attached to the gold shield. The target package and gold shield as well as the placement of pinhole backlighters and the two SPCAs can be seen in Fig. 1. The target package is placed at the center of the Omega chamber and each pinhole backlighter is perpendicular to the polyimide tube. The two backlighters are orthogonal to each other. The diagnostics are on the opposite side of the target from each pinhole backlighter.

The main diagnostic is dual, orthogonal, x-ray radiography. There are two pinhole backlighters each having a 5 mm square Ta foil with a stepped pinhole in the center. The step refers to a large hole on one side of the Ta and a smaller hole on the other. The pinhole backlighters are very sensitive to rotational alignment. Therefore, a stepped structure increases the size of the source while maintaining high resolution. The large opening is about 50 μm stepped to 20 μm. About 500 μm behind the pinhole is a 50 μm thick plastic square; attached to the rear of the plastic is a 500 μm square foil of either Ti or Sc. These foils are irradiated with 4 omega laser beams that have 200–400 J/beam, 1000–1200 μm spot size and a 1 ns square pulse. These beams overfill the metal foil, irradiating the plastic under the foil so that the expanding plastic provides radial tamping of the expanding metal plasma. The Sc and Ti create 4.09 and 4.51 keV x-rays, respectively. These x-rays pass through the pinhole in the Ta then pass through the target to the ungated DEF on the opposite side of the target.

On the rear surface of the polyimide piece, a 200 μm wide, 50–75 μm deep slot has been machined out of the plastic. A "tracer" strip of 4.3 at.% bromine doped plastic, $C_{500}H_{457}Br_{43}$ (CHBr), is glued into that slot. The CHBr has a density 1.42 g/cc. Since the CHBr and the polyimide have similar densities and are both predominately low Z materials, they will have similar evolutions in response to extreme pressures. The tracer strip is used because the bromine component of the CHBr more readily absorbs x-rays than the CH or polyimide; therefore, it provides contrast on the x-ray radiographs

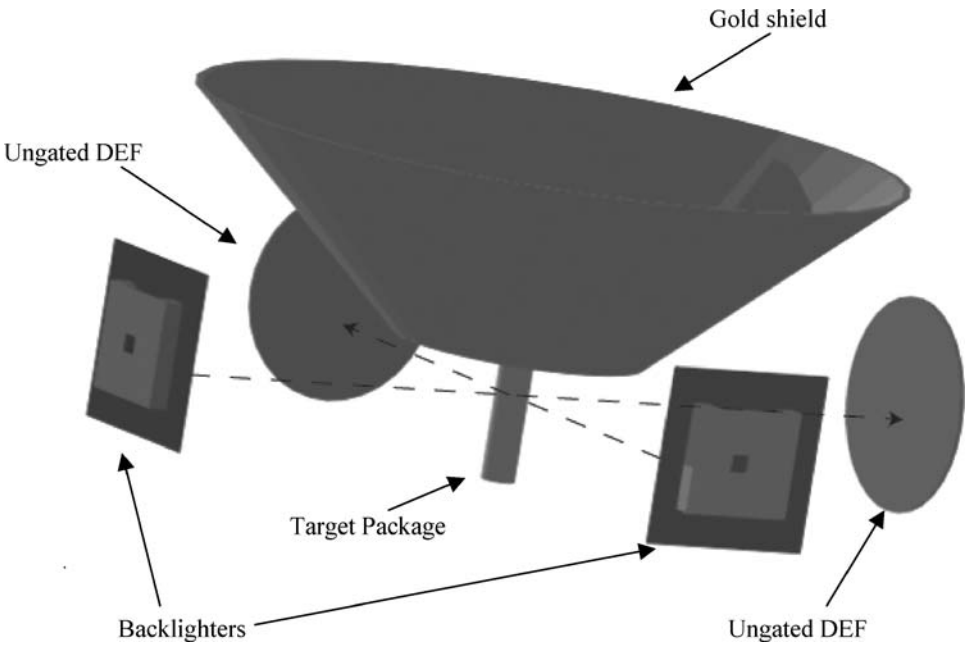

Fig. 1 Image of target with positions of backlighters and ungated detectors. Inside the polyimide tube attached to the gold shield contains a 150 μm plastic layer followed by a 2–3 mm CRF foam layer

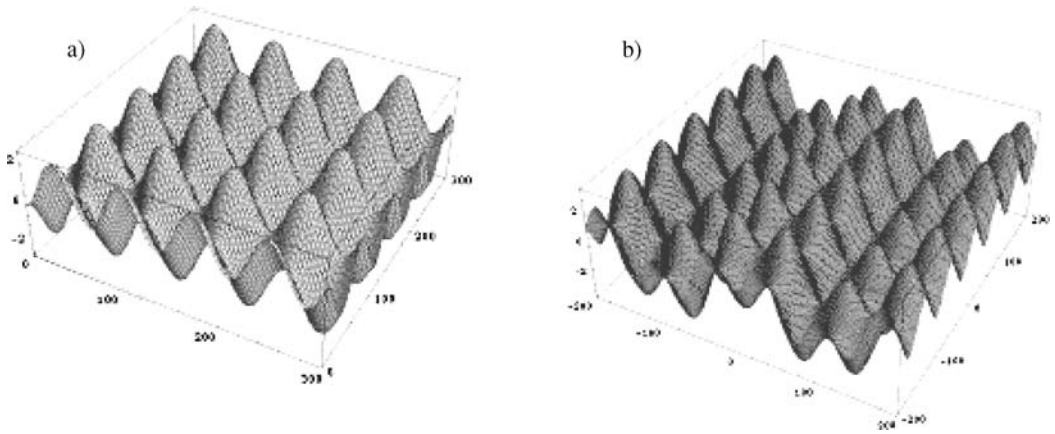

Fig. 2 (a) Single-mode perturbation, $a = 2.5\,\mu$m, $k = 2\pi/(71\,\mu\text{m})$. (b) 2-mode perturbation, $a = 2.5\,\mu$m, additional mode is $k = 2\pi/(212\,\mu\text{m})$

obtained by the primary diagnostics of the experiment. Also, since the strip is in the center of the target it allows the diagnostic to "look through" the polyimide since it is nearly transparent to the He-alpha x-rays used to diagnose the experiment. This allows the radiograph diagnose primarily the center of the target where the experiment is the least affected by target walls and sound waves created during the experiment.

After the tracer strip is in place a seed perturbation is machined onto the rear surface of the plastic component. This paper will discuss two types of perturbations. The basic pattern for both perturbations is two orthogonal sine waves with $a_0 = 2.5\,\mu$m and $k = 2\pi/(71\,\mu\text{m})$. The result is an "egg crate" pattern as seen in Fig. 2a, which will be referred to as a single-mode perturbation. The second type of perturbation has an additional mode whose wave vector is parallel to the long edge of the tracer strip. In this case, the additional mode has $a_0 = 2.5\,\mu$m and a $k = 2b\pi/(424\,\mu\text{m})$. This perturbation is referred as a 2-mode perturbation and can be seen in Fig. 2b. The reason to add additional modes is to explore enhanced spike penetration that these modes may produce. This has been seen in past experiments (Drake et al., 2004) and in simulations (Miles et al., 2003). This experiment uses dual, orthogonal radiography with one diagnostic line of sight down the tracer strip and the other across the tracer strip. The view across the strip allows one to see about 13 spikes on the radiograph and view down the strip allows one to see 3 or 4 spikes.

Results and discussion

Radiographs from recent experiments taken at 17 ns after the laser beams have fired can be seen in Fig. 3. Figure 3a is a radiograph of a single-mode target with the view across the tracer strip. Figure 3b is also a view across the tracer strip, but of a 2-mode target. The shock and interface are moving to the right in both images. Also, the tube walls are seen around $Y = \pm 470\,\mu$m and a gold grid is seen in each figure for calibration of magnification and position. In Fig. 3a there are several very bright lines due to scratches on the film. Notice that Fig. 3a has less contrast and more noise than Fig. 3b. This is because the radiograph in Fig. 3a is from a second layer DEF, where the first layer was overexposed and acted as a filter in this case. The resulting lineouts of this radiograph have been adjusted so that it is possible to compare relative positions between the two radiographs for the purposes of this paper.

The positions of notable features are more clearly seen in the horizontal lineouts taken from each radiograph seen in Fig. 4a and 4b for the single-mode and 2-mode cases, respectively. Two lineouts were taken for each radiograph in order to estimate the distance from the spike tip to bubble tip. One lineout was taken across a Rayleigh–Taylor spike, shown by the dark grey line, and the other across a bubble structure, shown by the black line. The location of each lineout is shown on the corresponding radiograph by a black rectangle. On each lineout the position of the shock, spike tip and bubble head are shown. The lineouts across the spike and bubble have a sharp decrease in intensity across the shock. Notice the sharp differences in the lineout across the spike as compared to the one across the bubble. The lineout across the spike then has a gradual decrease in intensity and then another abrupt decrease at the tip of the spike. The lineout across the bubble also has a gradual decrease in intensity after the shock followed by an abrupt decrease and then a gradual increase in intensity from the remaining plastic layer. However, the bubble has a higher intensity than the spike since it appears lighter in the radiograph. The sharp increased in intensity on the left portion of the single-mode lineout are from the scratches in the film mentioned earlier.

The positions of the shock, spike tip, and bubble head are shown by abrupt transitions in intensity, although the lineout shows them spread out over some horizontal distance. This is due to the finite resolution in experiment, the curvature of

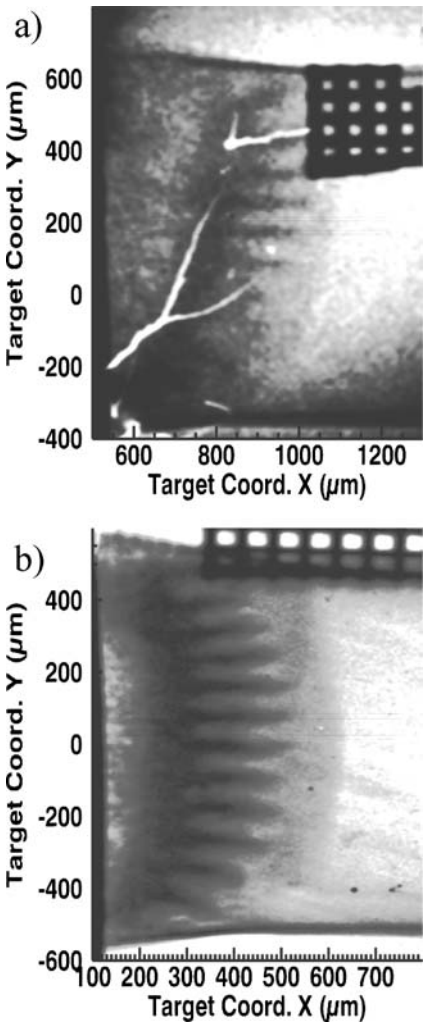

Fig. 3 Radiograph at 17 ns of (a) single-mode perturbation. (b) 2-mode perturbation

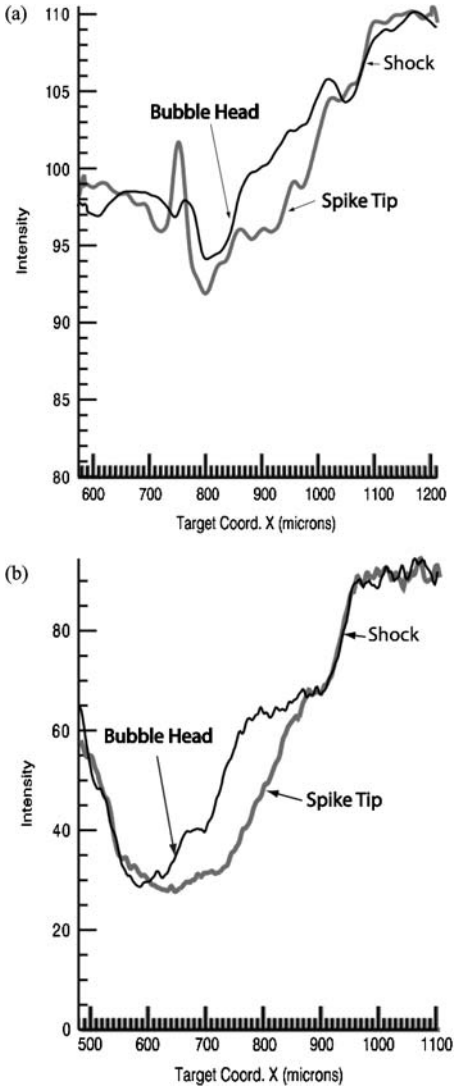

Fig. 4 (a) Lineouts at 17 ns across a spike and bubble in radiograph from single-mode perturbation and a (b) 2-mode perturbation

these features, and perhaps larger-scale variations in density and spike shape. In order to accurately and consistently define the locations of these features, a systematic method of analysis must be developed. The present, preliminary method involves finding the midpoint of the sharp decreases in intensity from the lineout in the portion determined to be the shock, spike tip or bubble head. The position of the bubble head is subtracted from the position of the spike tip to estimate the amplitude of the interface. At 17 ns, the amplitude of the single-mode perturbation is 143 μm and that of the 2-mode perturbation is 168 μm. The larger interface amplitude of the 2-mode perturbation is consistent with the results of simulations indicating that additional modes may cause increased growth (Miles et al., 2003). We are now working on the analysis required to subtract out the effects of refraction, which will be necessary to determine a meaningful growth rate for comparison with theory.

An additional radiograph can be seen in Fig. 5. This image is of a single-mode perturbation, but it is the view is down the tracer strip. Therefore, it is looking down 3 or 4 rows of about 13 spikes each. Note that on either side of the high contrast tracer strip are fainter spikes. These are spikes of the polyimide material surrounding the tracer strip. While polyimide is nearly transparent to the He-alpha x-rays used in this experiment, these spikes are a result of seeing an entire row of spikes aligned to be seen as one. For the same reason it is very difficult to see the location of the bubble head within the tracer strip. Looking through a row of $\sim$13 aligned spikes and bubbles causes a blurring of features in the radiograph. In contrast, the view across the tracer strip is only looking through $\sim$3 rows of aligned spikes and bubbles. The inaccuracy of the bubble head position in the view down the tracer strip can be seen from a lineout across the spike and bubble from the radiograph in Fig. 6. There is only a slight

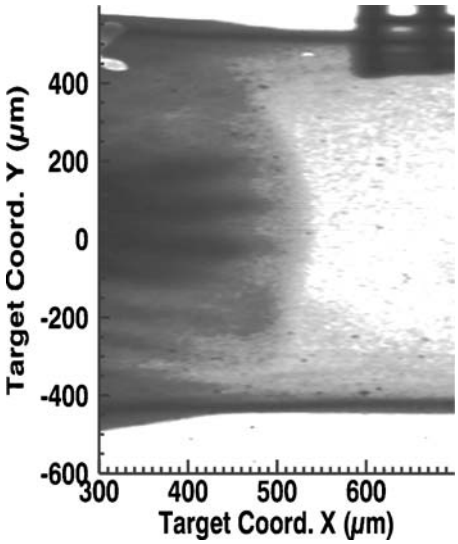

Fig. 5 Radiograph at 17 ns from single-mode perturbation down the strip view

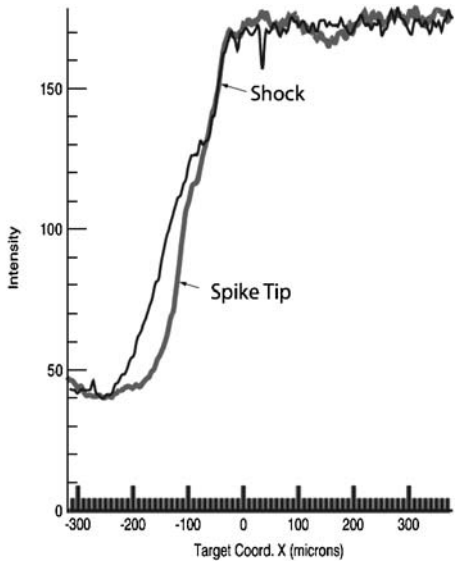

Fig. 6 (a) Lineout from radiograph at 17 ns of single-mode data across bubble and spike from a view down the strip as compared to (b) the across the strip view

difference in the lineouts of the bubble and spike, making it almost impossible to locate the bubble head. Compare these lineouts to the lineouts from a view across the strip for the same perturbation at the same time in Fig. 4a. Notice that the bubble position in the across the strip view is much more distinct than in the down the tracer strip view.

Conclusions

Recent experiments have been successful in obtaining data from targets well scaled to the expected conditions at the H/He interface in the explosion phase of SN1987A. Initial findings have shown that adding additional modes over the basic "egg crate" perturbation create larger amplitudes of the mixed layer. Dual, orthogonal radiography has allowed two views of the interface and the resulting growth of the mix layer from the Rayleigh–Taylor instability. Estimating this amplitude can be done by finding the positions of the spike tip and bubble head. This paper has shown that it is challenging to estimate the position of the bubble head in the view down the strip because many spikes form a line blurring its position. However, the bubble head position can be found more easily and more accurately from the view across the tracer strip. The view down the strip is still very useful for confirming the spike tip and shock position as well as diagnosing target abnormalities.

Acknowledgements The author would like to acknowledge Kai Ravariere, Aaron Miles, Dave Arnett, and Casey Meakin for their useful technical discussions. Financial support for this work included funding from the Stewardship Science Academic Alliances program through DOE Research Grant DE-FG03-99DP00284, and through DE-FG03–00SF22021 and other grants and contracts. This work is also supported in part by the U.S. Department of Energy under Grant No. B523820 to the Center for Astrophysical Thermonuclear Flashes at the University of Chicago.

References

Boehly, T.R., Craxton, R.S., et al.: Rev. Sci. Instr. **66**(1), 508 (1995)
Drake, R.P., Leibrandt, D.R., et al.: Phys. Plasmas **11**(5), 2829 (2004)
Kane, J., Arnett, D., et al.: ApJ **528**, 989 (2000)
Meshkov, E.E.: Fluid Dyn. **4**, 101 (1969)
Miles, A.R., Edwards, M.J., et al.: The Effect of a Short-wavelength Mode on the Nonlinear Evolution of a Long-wavelength Perturbation Driven by a Strong Blast Wave. Inertial Fusion and Science Applications, Monterey, CA (2003)
Rayleigh, L.: Scientific Papers II. Cambridge, England, Cambridge (1900)
Remington, B.A., Drake, R.P., et al.: Phys. Plasmas **7**(May), 1641 (2000)
Richtmyer, D.H.: Commun. Pure Appl. Math. **13**, 297 (1960)
Robey, H.F., Kane, J.O., et al.: Phys. Plasmas **8**, 2446 (2001)
Ryutov, D.D., Drake, R.P., et al.: ApJ **518**(2), 821 (1999)
Taylor, S.G.: Proc. R. Soc. **A201**, 192 (1950)